Chinese Journal of Catalysis 39 (2018) 1121–1128

available at www.sciencedirect.com

ScienceDirect

journal homepage: www.elsevier.com/locate/chnjc

Article

Glycerol hydrogenolysis to *n*-propanol over Zr-Al composite oxide-supported Pt catalysts

Chuang Li [a], Bo He [a], Yu Ling [a], Chi-Wing Tsang [b], Changhai Liang [a,*]

[a] *Laboratory of Advanced Materials and Catalytic Engineering, Dalian University of Technology, Dalian 116024, Liaoning, China*
[b] *Faculty of Science and Technology, Technological and Higher Education Institute of Hong Kong, Hong Kong 50011, China*

ARTICLE INFO

Article history:
Received 29 January 2018
Accepted 22 March 2018
Published 5 June 2018

Keywords:
Glycerol hydrogenolysis
n-Propanol
Pt-based catalyst
Zr-Al composite oxide
Zr/Al ratio

ABSTRACT

Zr-Al mixed oxide supported Pt catalysts with different Zr/Al mole ratios (2.5%Pt/$Zr_xAl_{1-x}O_y$) were synthesized by an impregnation method and used for the selective hydrogenolysis of glycerol to *n*-propanol in an autoclave reactor. The catalysts were fully characterized by X-ray powder diffraction, Brunauer-Emmett-Teller surface area analysis, CO chemisorption, H_2 temperature-programmed reduction, pyridine-infrared spectroscopy, and NH_3-temperature-programmed desorption. The results revealed that the Zr/Al ratio on the support significantly affected the size of the platinum particles and the properties of the acid sites on the catalysts. The catalytic performance was well correlated with the acidic properties of the catalyst; specifically, more acid sites contributed to the conversion and strong acid sites with a specific intensity contributed to the deep dehydration of glycerol to form *n*-propanol. Among the tested catalysts, 2.5 wt% Pt/$Zr_{0.7}Al_{0.3}O_y$ exhibited excellent selectivity for *n*-propanol with 81.2% glycerol conversion at 240 °C and 6.0 MPa H_2 pressure when 10% aqueous glycerol solution was used as the substrate. In addition, the effect of various reaction parameters, such as H_2 content, reaction temperature, reaction time, and number of experimental cycles were studied to determine the optimized reaction conditions and to evaluate the stability of the catalyst.

1. Introduction

In recent years, the vast amounts of glycerol generated by biodiesel refineries motivated research on the development of new ways to transform glycerol into high value-added chemicals [1]. Catalytic hydrogenolysis is one of the most attractive ways in this context [2,3]. Up to now, research on the hydrogenolysis of glycerol was mainly focused on its conversion to diols such as 1,2-propandiol (1,2-PD) or 1,3-propandiol (1,3-PD) [4–9]. *n*-Propanol (*n*-PO) is another valuable chemical produced during the hydrogenolysis of glycerol; however, the direct conversion of glycerol to *n*-PO remains essentially unexplored. Few researchers have studied the direct conversion of glycerol to n-propanol, despite the fact that *n*-propanol is relatively expensive (price: 1,3-propandiol > *n*-propanol > 1,2-propandiol > ethylene glycol [10]). Further, *n*-propanol is a valuable chemical widely used as a solvent, organic intermediate, and raw material [11,12]. In addition to the one-pot hydrodeoxygenation of glycerol to propylene in a batch reactor [13,14], single-step [15] and tandem processes [16,17] of glycerol to olefins (GTO) in H_2 have been developed by first converting the dehydration products (mainly acrolein and acetol)

---

* Corresponding author. Tel/Fax: +86-411-84986353; E-mail: changhai@dlut.edu.cn

This work was supported by the National Natural Science Foundation of China (21573031, 21373038), the Program for Excellent Talents in Dalian City (2016RD09), and the Doctoral Scientific Research Foundation of Liao Ning Province (20170520395).

DOI: 10.1016/S1872-2067(18)63068-2 | http://www.sciencedirect.com/science/journal/18722067 | Chin. J. Catal., Vol. 39, No. 6, June 2018

to propanols and then to propylene.

At present, research on glycerol hydrogenolysis to *n*-propanol is mainly focused on improving the acidity of catalysts to promote their dehydration ability. Zhu et al. [12] reported a one-step hydrogenolysis of biomass-derived glycerol to propanol over different supported Pt-$H_4SiW_{12}O_{40}$ (HSiW) bi-functional catalysts in aqueous media. It was believed that the balance between the active sites and acid sites is important for glycerol conversion. Later, Samudral et al. [18] compared different heteropolyacids in the Pt-HPA/ZrO_2 catalyst series and found that Pt-$H_4SiW_{12}O_{40}$/ZrO_2 exhibited the highest propanol (*n*-propanol and *i*-propanol) yield. Its high activity was attributed to the greater dispersion of Pt particles and stronger acidity of the support. Guo et al. [19] found that mesoporous niobium tungsten oxide-supported platinum exhibited good propane selectivity, but the complex synthesis process of the catalyst hampers its industrial application. In addition, it was found that changes in the acidity of the catalyst could significantly affect product distribution when 10Ni-30H_4SiW/Al_2O_3 was used in the reaction, in which Cs^+ can be exchanged to alter the acidity of the catalyst [10]. In spite of previous research efforts, the specific relationship between hydrogenolysis product distribution and acidity of the catalyst is still not clear and needs to be evaluated.

Combined ZrO_2 is often used as a carrier during glycerol hydrogenolysis to propanol owing to the fact that the composite metal oxide has stronger acidity, higher specific surface area, and better stability than a single-component oxide [20–23]. In this study, Zr-Al composite oxides with different ratios were synthesized and an impregnation method was employed to use them as supports for platinum catalysts. These catalysts were then applied during glycerol hydrogenolysis to explore the effect of the supports on the transformation of glycerol to *n*-propanol. The effects of H_2 content, reaction temperature, reaction time, and catalyst stability were also examined.

2. Experimental

2.1. Preparation of Zr-Al mixed oxide-supported Pt catalysts

Zr-Al composite oxides with different Zr/Al ratios were prepared by the co-precipitation method. In a general process, $ZrOCl_2\cdot 8H_2O$ and $Al(NO_3)_3\cdot 9H_2O$ with different mole ratios were dissolved in deionized water (120 mL) at room temperature. To the resulting transparent solution, aqueous ammonia (25%–28%) was dropwise added under vigorous stirring until the solution became a gel-like solid. The white gel solid was aged at room temperature for 12 h, filtered, and washed with deionized water until no chloride ions could be detected against an $AgNO_3$ solution. The resulting precipitate was dried at 110 °C for 12 h and then calcined at 400 °C for 4 h. Similarly, Zr-Al composite oxides with different metal ratios were prepared and denoted as $Zr_xAl_{1-x}O_y$ (x and $1-x$ represent the mole ratios of Zr and Al respectively, x = 0.3, 0.5, and 0.7; y stands for the uncertain value of oxygen element). For comparison, single oxide Al_2O_3 and ZrO_2 were also synthesized by the same procedure.

Zr-Al composite oxide-supported platinum catalysts were prepared by a wet impregnation method. An aqueous solution of $H_2PtCl_6\cdot 6H_2O$ was impregnated with required amounts of different Zr-Al composite oxides individually under vigorous stirring for 24 h. After rotary evaporation, the impregnated samples were allowed to dry overnight at 110 °C and the resulting materials were calcined at 350 °C for 4 h. Platinum loading in all the catalysts was fixed at 2.5 wt% and the catalysts were denoted as 2.5%Pt/ZrO_2, 2.5%Pt/$Zr_{0.3}Al_{0.7}O_y$, 2.5%Pt/$Zr_{0.5}Al_{0.5}O_y$, 2.5%Pt/$Zr_{0.7}Al_{0.3}O_y$, and 2.5%Pt/Al_2O_3.

2.2. Catalytic reaction tests

The hydrogenolysis reaction was carried out in a Hastelloy Alloy autoclave. Prior to the reaction, the catalyst was reduced by 25% H_2 in an Ar atmosphere (flowing at a rate of 60 mL/min) at 350 °C for 4 h. For each reaction, the standard experimental conditions were as follows: initial H_2 pressure of 6 MPa, temperature of 230 °C, stirring speed of 800 r/min, and reaction time of 8 h. In a typical reaction, 30 g of a 10% glycerol solution and 0.3 g of the catalyst were loaded into the reactor, after which the autoclave was sealed and flushed thrice with H_2 to remove the air in the reactor. After the reaction temperature reached the designated value, the reaction began. At the end of the reaction, the liquid products were analyzed using a gas chromatograph (7890F GC) equipped with a capillary column (FFAP: 30 m × 0.32 mm × 0.5 μm) and a flame ionization detector. *n*-Butanol was used as the internal standard.

2.3. Characterization

Powder X-ray diffraction (XRD) data were recorded on a Shimadzu XRD-7000S diffractometer with a Cu K_α monochromatized radiation source (λ = 1.5418 Å), which is operated at 40 kV and 30 mA. The diffraction data were collected in a continuous scanning mode at a scan speed of 3°/min in the 2θ range of 5° to 90°.

N_2 adsorption-desorption isotherms were generated on a Quantachrome Autosorb-iQ-C instrument. Before the N_2 physisorption measurements, all the samples (approximately 0.1 g) were heated to 300 °C in vacuum (10^{-3} Torr) for 3 h to remove any adsorbed impurities. Later, the experiment was performed at −196 °C.

The quantities of metal active sites were estimated from CO adsorption analysis performed using a Micrometer Autochem 2910 instrument at room temperature. In a typical process, the catalyst was reduced in flowing H_2 (30 mL/min) at 350 °C for 2 h, followed by purging with flowing He for 2 h. Subsequently, CO was pulsed until the peak area did not change anymore at room temperature.

For the temperature-programmed reduction of H_2 (H_2-TPR), the catalysts (50 mg) were subjected to a flow of 10% (volume fraction) H_2/Ar (total flow rate of 30 mL/min) for 1 h to stabilize the thermal conductivity detector (TCD) signal. After that, the temperature was increased from 30 to 450 °C at a rate of 10 °C/min. The temperature-dependent changes in the concentration of H_2 were recorded on an on-line TCD.

The acidity of the reduced catalyst was measured by the NH_3-temperature-programmed desorption (NH_3-TPD) technique. Prior to NH_3 adsorption, the sample was outgassed at 200 °C for 1 h in order to remove the impurities on the catalyst surface. After cooling down to 50 °C in a He flow, NH_3 adsorption was carried out (30 mL/min) for 40 min. Physisorbed ammonia was eliminated by flowing He for 1 h. NH_3-TPD was performed in He flow at a temperature ramp of 10 °C/min from 50 to 800 °C on a Quantachrome Instruments Chembet 3000 system.

3. Results and discussion

3.1. Characterization of 2.5%Pt/$Zr_xAl_{1-x}O_y$ catalysts

Fig. 1. shows the XRD patterns of 2.5%Pt/$Zr_xAl_{1-x}O_y$ catalysts reduced at 350 °C. First, diffraction peaks corresponding to the Pt metal particles were only detected in the case of 2.5%Pt/$Zr_{0.7}Al_{0.3}O_y$ and 2.5%Pt/$Zr_{0.5}Al_{0.5}O_y$. Moreover, based on the intensities of the XRD peaks, the size of the Pt particles in the 2.5%Pt/$Zr_{0.7}Al_{0.3}O_y$ catalyst was large compared to 2.5%Pt/$Zr_{0.5}Al_{0.5}O_y$; further, the Pt particles were well dispersed on the other three catalysts [24]. The diffraction peaks of 2.5%Pt/ZrO_2 and 2.5%Pt/Al_2O_3 were attributed to orthorhombic ZrO_2 (JCPDS No. 34-1084) and hexagonal Al_2O_3 (JCPDS No. 13-0373), respectively. However, the catalysts exhibited low crystallinities, which could be attributed to the low calcination temperatures. In the case of Zr-Al oxide-supported Pt catalysts, 2.5%Pt/$Zr_xAl_{1-x}O_y$ (x = 0.3, 0.5, and 0.7), the XRD peaks were almost similar, with the emergence of a broad peak near 32°; however, the positions of the Pt particle peaks were different. There were no peaks corresponding to single phase zirconia or alumina, which indicated that the alumina and zirconia components were combined uniformly to form composite metal oxides [25].

The specific surface areas and dispersions of metal active sites are shown in Table 1. It is to be noted that the specific surface areas and pore volumes increased with an increase in the Al content. As for 2.5%Pt/ZrO_2, the largest pore size (25.7 nm) could be attributed to the accumulation of spherical ZrO_2 particles. The dispersion of Pt particles ranged widely from 19.0% to 34.8%, while the particle size ranged from 3.4 to 6.2 nm. The catalysts, 2.5%Pt/$Zr_{0.7}Al_{0.3}O_y$ and 2.5%Pt/$Zr_{0.5}Al_{0.5}O_y$, exhibited larger Pt particles, 6.2 and 5.0 nm, respectively, which is consistent with the XRD results. The active sites of larger Pt particles may affect the selectivity of n-propanol.

Table 1
Pore structure characteristics and dispersion of the metal active sites of 2.5%Pt/$Zr_xAl_{1-x}O_y$ catalysts with different Zr/Al ratios.

Catalyst	S_{BET} [a] (m²/g)	V_p [a] (cm³/g)	d_p [a] (nm)	Dis [b] (%)	P_d [b] (nm)
2.5%Pt/ZrO_2	65	0.067	25.7	30.3	3.9
2.5%Pt/$Zr_{0.7}Al_{0.3}O_y$	67	0.087	4.3	19.0	6.2
2.5%Pt/$Zr_{0.5}Al_{0.5}O_y$	87	0.081	3.7	23.6	5.0
2.5%Pt/$Zr_{0.3}Al_{0.7}O_y$	120	0.090	10.2	30.1	3.9
2.5%Pt/Al_2O_3	265	0.110	8.9	34.8	3.4

[a] Measured by N_2 adsorption-desorption isotherms.
[b] Calculated by CO chemisorption.

The Zr-Al composite oxide-supported Pt catalysts were studied by H_2-TPR as shown in Fig. 2. It was reported that the active sites highly dispersed on catalyst surfaces have a strong interaction with the support and that the reduction temperatures under such conditions would be higher [27,28]. Therefore, it could be deduced from the reduction temperatures of 2.5%Pt/Al_2O_3, 2.5%Pt/$Zr_{0.3}Al_{0.7}O_y$, and 2.5%Pt/ZrO_2 catalysts that 2.5%Pt/Al_2O_3 exhibited a higher metal dispersion. While in the case of 2.5%Pt/$Zr_{0.5}Al_{0.5}O_y$ and 2.5%Pt/$Zr_{0.7}Al_{0.3}O_y$ catalysts, they displayed two reduction peaks, one near 125 °C and the other near 325 °C. This indicates that the catalysts contained active ingredients of two different sizes. The lower temperature reduction peak was attributed to the bigger particles that interacted weakly with the support [29]. The reduction peak at 325 °C could be ascribed to smaller Pt oxides, which were highly dispersed on the support. The H_2-TPR results were consistent with the results of XRD and CO chemisorption analyses.

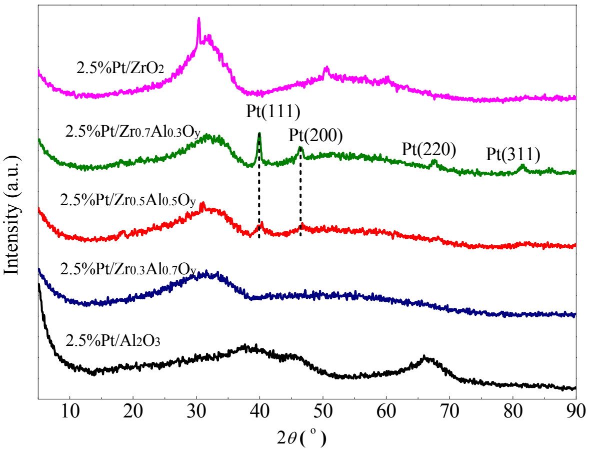

Fig. 1. XRD patterns of 2.5%Pt/$Zr_xAl_{1-x}O_y$ catalysts with different Zr-Al ratios.

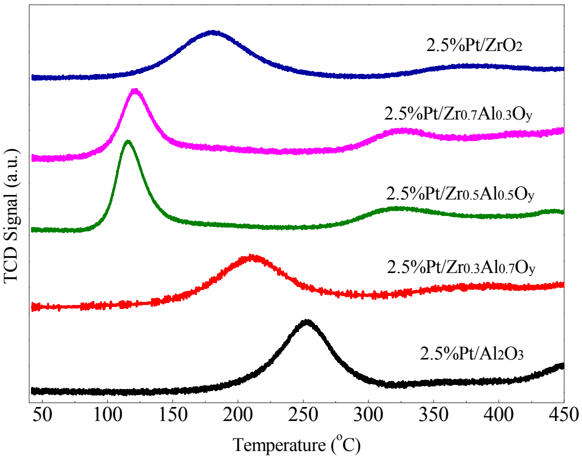

Fig. 2. H_2-TPR profiles of 2.5%Pt/$Zr_xAl_{1-x}O_y$ catalysts with different Zr/Al ratios.

To further elucidate the types of acids on the catalysts and the ratio of strong Brönsted to Lewis acid sites, pyridine adsorption analysis was carried out and the collected spectra are presented in Fig. 3. The results clearly showed that the acid sites were mainly Lewis acids on the 2.5%Pt/$Zr_xAl_{1-x}O_y$ catalysts. Briefly, the intense peak at 1450 cm^{-1} was assigned to pyridine adsorption on Lewis acid sites. Another comparatively lesser band at 1541 cm^{-1}, due to the N-H bending of pyridinium ions, is the characteristic adsorption peak of pyridine on Brönsted acid sites. The peak located at 1490 cm^{-1} was attributed to the combination adsorption of pyridine molecules on both Brönsted and Lewis acid sites [30]. To investigate the effect of different Zr/Al mole ratios on the surface acidity of the as-synthesized 2.5%Pt/$Zr_xAl_{1-x}O_y$ catalysts, NH_3-TPD was carried out and the results are shown in Fig. 4. In pure oxide-supported catalysts, such as 2.5%Pt/ZrO_2 and 2.5%Pt/Al_2O_3, the acid distribution was uniform. Weak, medium strength, and strong acid sites existed on the surfaces of the catalysts. When using Zr-Al composite oxides as the supports, such as in the case of 2.5%Pt/$Zr_{0.3}Al_{0.7}O_y$, NH_3 desorption peaks located at lower temperatures decreased and the acid distributions transferred to stronger acid sites. Such changes in this trend were confirmed with increasing Zr/Al mole ratios. There are no weak acid sites on the 2.5%Pt/$Zr_{0.5}Al_{0.5}O_y$ catalyst and in the case of 2.5%Pt/$Zr_{0.7}Al_{0.3}O_y$, the percentage of strong acid exhibited a maximum value of 91.2%. In addition, the desorption peak of the 2.5%Pt/$Zr_{0.7}Al_{0.3}O_y$ catalyst became much sharper and intensified, which indicated that the strong acid sites were more in number [25]. They would contribute to an improvement in the product selectivity [10].

For ease of analysis, the acid sites were classified as weak acid, medium strong acid, and strong acid sites when the desorption temperatures were <200, 200–450, and >450 °C, respectively. The distributions of acid sites and percentages of the single peak at the NH_3 desorption temperature of 580 °C were calculated by peak fitting (Table 2). In addition, it is worth noting that the total number of acid sites increased with an increase in the Al content, which would be beneficial for the conversion of glycerol.

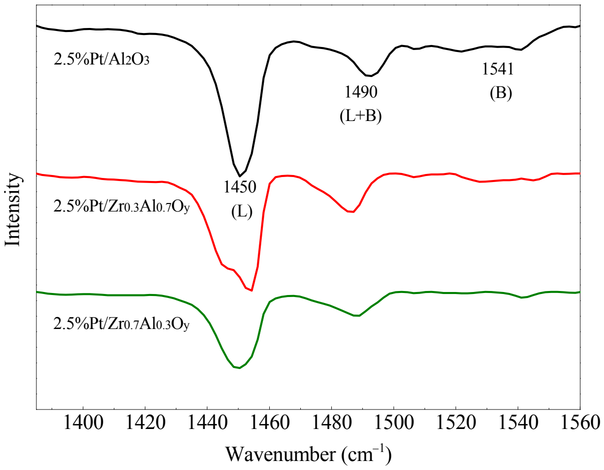

Fig. 3. FT-IR spectra of adsorbed pyridine on 2.5%Pt/$Zr_xAl_{1-x}O_y$ catalysts with different Zr/Al ratios (desorption at 300 °C).

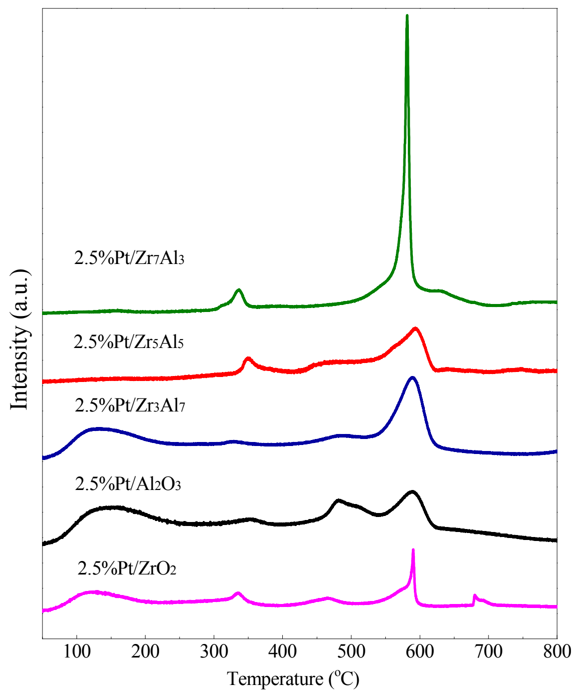

Fig. 4. NH_3-TPD profiles of Zr-Al composite oxide-supported platinum catalysts with different Zr/Al ratios.

3.2. *Hydrogenolysis of glycerol over supported catalysts*

The synthesized catalysts were used for the hydrogenolysis of glycerol and the effect of different Zr/Al ratios on the reaction was investigated. The results are shown in Table 3. Based on available literature [32] and our experimental results, a possible reaction route for glycerol hydrogenolysis is proposed. Acid-catalyzed dehydration of glycerol initially proceeds to form acetol or 3-hydroxypropionaldehyde, which can subsequently hydrogenate to 1,2-PD and 1,3-PD over metal catalysts, respectively. As shown in Table 3, a higher selectivity for 1,3-PD than 1,2-PD on Pt/ZrO_2 and Pt/$Zr_{0.7}Al_{0.3}O_y$ is obvious; meanwhile, higher selectivity can be found for 1,2-PD on Pt/$Zr_{0.5}Al_{0.5}O_y$, Pt/$Zr_{0.3}Al_{0.7}O_y$, and Pt/Al_2O_3. This seems to indicate that *n*-PO is formed mainly by further hydrogenolysis of 1,3-PD over Pt/ZrO_2 and Pt/$Zr_{0.7}Al_{0.3}O_y$. Formation of 1,3-PD via glycerol hydrogenolysis requires the selective cleavage of a secondary hydroxy group among the three hydroxy groups of a

Table 2
Acid site distribution on 2.5%Pt/$Zr_xAl_{1-x}O_y$ catalysts.

Catalyst	Acid strength distribution (%)				n_T [a] (mmol/g)
	W [a]	M [a]	S [a]	Single peak [b] (580 °C)	
2.5%Pt/ZrO_2	16.3	17.0	66.7	54.2	1.77
2.5%Pt/$Zr_{0.7}Al_{0.3}O_y$	0.0	8.8	91.2	91.2	2.87
2.5%Pt/$Zr_{0.5}Al_{0.5}O_y$	0.0	12.8	87.2	52.5	3.58
2.5%Pt/$Zr_{0.3}Al_{0.7}O_y$	37.8	8.4	53.7	37.8	4.78
2.5%Pt/Al_2O_3	45.0	9.5	45.5	20.2	6.27

[a] W, M, S, and n_T stand for the number of weak, medium, strong, and total acid sites, respectively. [b] The percentage of acid sites, whose NH_3 desorption temperature is 580 °C.

Table 3
Hydrogenolysis of glycerol over Zr-Al composite oxide-supported Pt catalysts.

Entry	Catalyst	Conv. (%)	Selectivity (%)							
			n-PO	1,2-PD	*i*-PO	1,3-PD	EG	MA	EA	Others
1	2.5%Pt/ZrO_2	26.4	75.4	3.1	14.6	4.9	1.3	0.3	0.2	0.2
2	2.5%Pt/$Zr_{0.7}Al_{0.3}O_y$	34.2	82.7	4.3	4.7	6.4	0.8	0.2	0.5	0.4
3	2.5%Pt/$Zr_{0.5}Al_{0.5}O_y$	38.0	53.9	2.8	36.7	1.3	1.3	1.6	1.4	1.0
4	2.5%Pt/$Zr_{0.3}Al_{0.7}O_y$	38.4	41.9	45.3	3.9	2.9	4.5	1.3	–	0.2
5	2.5%Pt/Al_2O_3	38.9	36.3	48.4	6.4	3.4	3.7	0.3	0.8	0.7

Reaction conditions: 10% glycerol solution; $m_{catalyst}$:$m_{glycerol}$ = 1:10; H_2 volume: 20 mL; Temperature: 230 °C; Time: 8 h; H_2 pressure: 6.0 MPa.
n-PO = *s*-propanol; 1,2-PD = 1,2-propanediol; *i*-PO = *i*-propanol; 1,3-PD = 1,3-propanediol; EG = ethylene glycol; MA = methanol; EA = ethanol.

glycerol molecule. Brønsted acid sites are more advantageous than Lewis acid sites for the selective conversion of glycerol to 1,3-propanediol, as reported in literature [33]. In order to elucidate the reaction sequence of glycerol hydrogenolysis, the hydrogenolysis of 1,2-PD and 1,3-PD over 2.5%Pt/$Zr_{0.7}Al_{0.3}O_y$ was evaluated under conditions similar to those of glycerol hydrogenolysis. The conversion of 1,2-PD is much higher than that of 1,3-PDO. 1,2-PD was efficiently transformed to yield *n*-PD and *i*-PD. It is confirmed that propanediols can undergo further sequential hydrogenolysis to form *n*-PD and *i*-PD. When dehydration occurs at the central hydroxyl group of 1,2-PD or the terminal hydroxyl group of 1,3-PD, propanal is produced and subsequently hydrogenates to form *n*-PO. In contrast, when dehydration occurs at the terminal hydroxyl group of 1,2-PDO, acetone is produced, which is then further hydrogenated to yield *i*-PO. Meanwhile, high selectivities for *i*-PO and 1,2-PD could be found on Pt/$Zr_{0.5}Al_{0.5}O_y$ and Pt/$Zr_{0.3}Al_{0.7}O_y$, respectively, indicating that a proper balance of strong, moderate, and weakly acidic sites is responsible for the selective hydrogenolysis of glycerol to *i*-PO or 1,2-PD. Ethylene glycol can also be obtained by glycerol hydrogenolysis. However, it was not detected in 1,2-PD and 1,3-PD hydrogenolysis, indicating that ethylene glycol was produced directly from glycerol by a C–C bond cleavage reaction. Due to the reaction between glycerol and 1,2-PD, ethanol, which might be formed via the sequential hydrogenolysis of ethylene glycol or decomposition of 1,2-PDO, was observed. Finally, the other product, methanol, was formed through overhydrogenolysis or decomposition reactions. When using 2.5%Pt/ZrO_2 as the catalyst, the selectivity of *n*-propanol was 75.4%, while glycerol conversion was only 26.4%. By Al doping of the support, the conversion and selectivity of the reactions could be altered. In order to further analyze the effect of aluminum content on glycerol conversion, glycerol conversion and the acid amounts of different catalysts were calculated, as shown in Fig. 5. It was found that glycerol conversion increased with an increase in the amount of the total acid sites on the catalysts. Some studies pointed out that acid sites can promote the dehydration of glycerol [18,31]. Hence, the increase observed in glycerol conversion by increasing the aluminum content was attributed to the improvement in surface acidity. When Al/Zr was more than 1:1, glycerol conversion was no longer promoted; this observation can be attributed to other factors, such as temperature, glycerol concentration, hydrogen content, and the number of active sites.

As for the reactions catalyzed by 2.5%Pt/Al_2O_3 and 2.5%Pt/$Zr_{0.3}Al_{0.7}O_y$ (Table 3, entries 4 and 5), the selectivity for 1,2-propanediol was higher than that for *n*-propanol. The presence of 1,2-propanediol may be related to the weak acid sites on the surfaces of the catalysts. The weak acid sites could only remove one hydroxyl group to a certain extent. The reaction catalyzed by those catalysts whose Zr/Al mole ratio is more than 1:1, such as 2.5%Pt/$Zr_{0.5}Al_{0.5}O_y$, 2.5%Pt/$Zr_{0.7}Al_{0.3}O_y$, and 2.5%Pt/ZrO_2, exhibited higher selectivity for propanol; the selectivity for propanol (*n*-propanol + *i*-propanol) was more than 87%. Combining these results, it was concluded that these three catalysts had a large number of strong acid sites (Table 2). The higher selectivity for propanol may be ascribed to the strong dehydration properties of the strong acid sites. This phenomenon indicates that the acidity of catalyst surface affects the degree of dehydroxylation in glycerol. Strong acids promote the deep dehydration of glycerol to form greater quantities of propanol; this result correlates well with previous studies [31].

Although the total values of propanol (*n*-propanol + *i*-propanol) selectivity catalyzed by 2.5%Pt/$Zr_{0.5}Al_{0.5}O_y$, 2.5%Pt/$Zr_{0.7}Al_{0.3}O_y$, and 2.5%Pt/ZrO_2 were almost the same, the *n*-propanol selectivity values were different. Among them, the maximum selectivity for *n*-propanol (82.7%) was achieved when 2.5%Pt/$Zr_{0.7}Al_{0.3}O_y$ was used as the catalyst. Combined with the NH_3-TPD analysis, it could be observed that the 2.5%Pt/$Zr_{0.7}Al_{0.3}O_y$ catalyst exhibited the largest NH_3 desorption peak at around 580 °C. This indicated that the selectivity of *n*-propanol may be associated with the acid sites at 580 °C. Fig. 6. shows the relationship between *n*-propanol selectivity and

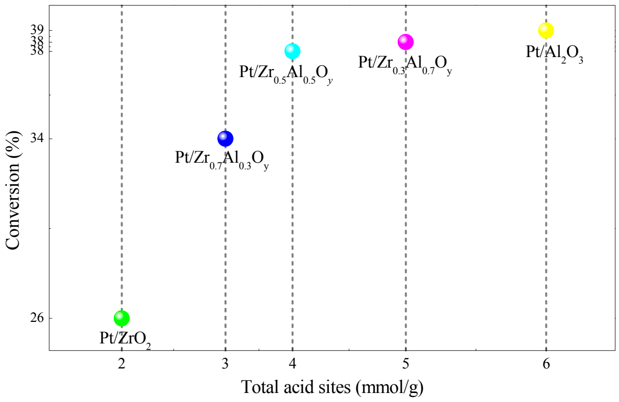

Fig. 5. Relationship between glycerol conversion and the total acid amount on the catalyst surfaces.

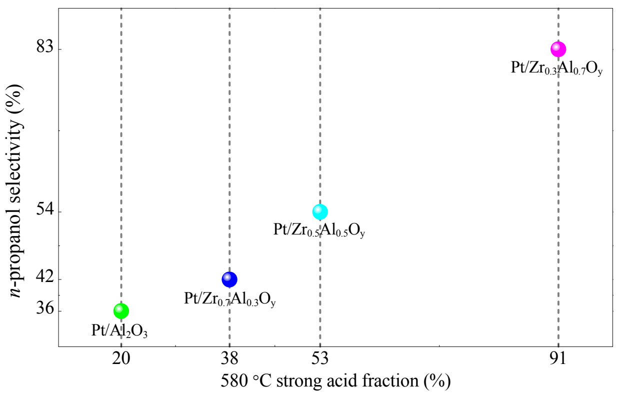

Fig. 6. Relationship between the selectivity for *n*-propanol and the percentage of acid sites whose NH_3 desorption peak is around 580 °C.

the percentage of acid sites whose NH_3 desorption temperature is around 580 °C. It was found that the selectivity for *n*-propanol was almost linearly related to the percentage of acids. Some researchers also pointed out that *n*-propanol selectivity was related to strong acid sites of a specific intensity on the catalyst [10]. The location corresponds to a specific acid site that is beneficial for the transformation of glycerol to *n*-propanol on the catalyst.

Based on the results described above, 2.5%$Pt/Zr_{0.7}Al_{0.3}O_y$ was chosen as the catalyst to examine the influence of reaction conditions, such as hydrogen content, reaction temperature, and reaction time, on the glycerol hydrogenolysis reaction. The results are included in the Supporting Information. The results showed that an increase in the H_2 amount, reaction temperature, or reaction time could significantly promote the conversion of glycerol. About 81.2% of glycerol conversion and 86.3% of *n*-propanol selectivity were obtained under the reaction conditions of 240 °C, 8 h, and 35 mL H_2.

To evaluate the reusability of the 2.5%$Pt/Zr_{0.7}Al_{0.3}O_y$ catalyst, the used catalyst was first washed several times with deionized water and then calcined in a tube furnace at 300 °C for 2 h, followed by reduction in H_2 flow at 350 °C for 4 h. Later, the catalyst was used for a second round under the same reaction conditions. The results of reusability analysis are shown in Fig. 7. After being used for 5 times, the catalyst still led to almost the same glycerol conversion percentage. However, the selectivity of *n*-propanol decreased slightly, while that of *i*-propanol began to increase.

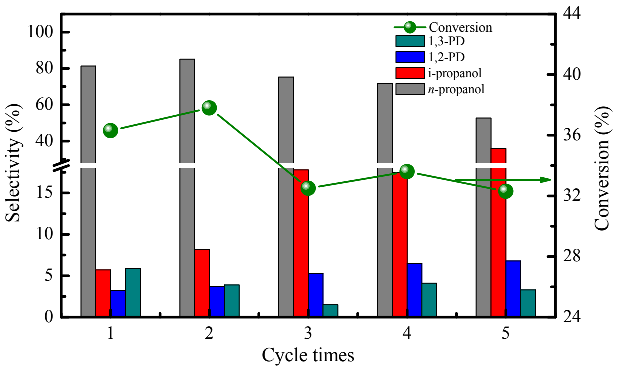

Fig. 7. Reusability of 2.5%$Pt/Zr_{0.7}Al_{0.3}O_y$ catalyst for glycerol hydrogenolysis. Reaction conditions: 10% glycerol solution; $m_{catalyst}$:$m_{glycerol}$ = 1:10 H_2 volume: 20 mL; Temperature: 230 °C; Time: 8 h; H_2 pressure: 6.0MPa.

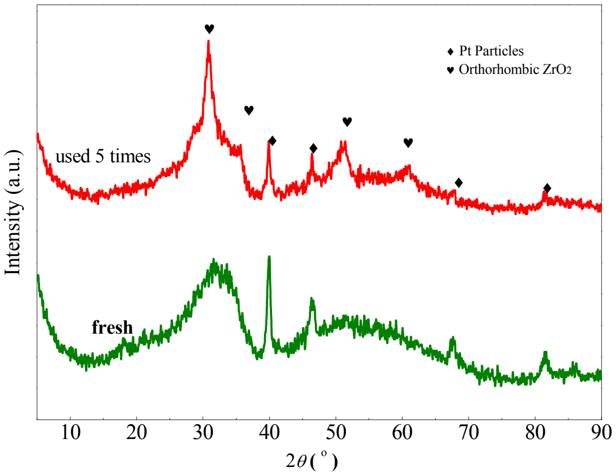

Fig. 8. XRD patterns of fresh and used 2.5%$Pt/Zr_{0.7}Al_{0.3}O_y$ catalysts.

In order to explain these phenomena, the catalyst used 5 times was analyzed by XRD and NH_3-TPD analyses (shown in Fig. 8 and Fig. 9, respectively). It can be clearly observed that the XRD peaks of the 2.5%$Pt/Zr_{0.7}Al_{0.3}O_y$ catalyst are very different from those of the catalyst used 5 times; peaks corresponding to orthorhombic ZrO_2 (JCPDS No. 34-1084) were observable in the XRD pattern of the catalyst used 5 times. No apparent leaching of Pt and Al could be detected in the residual solution by inductively coupled plasma-atomic emission spectroscopy (ICP-AES) though partially orthorhombic ZrO_2 separated out from the Zr-Al composite oxide, which may due to the calcination of the catalyst and reduction at high temperatures. As shown in the NH_3-TPD results, the total number of acid sites were almost similar for the fresh and used catalysts, 2.87 and

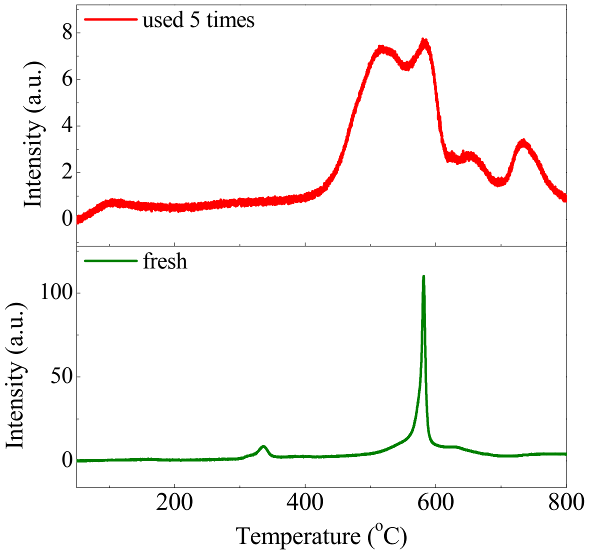

Fig. 9. NH_3-TPD profiles of fresh and used 2.5%$Pt/Zr_{0.7}Al_{0.3}O_y$ catalysts.

2.81 mmol/g, respectively. However, the acid site distribution on the catalyst surfaces varied greatly. Fig. 9 shows that the NH_3 desorption peak appeared at a lower temperature for the used catalyst and the percentage of acid sites whose NH_3 desorption temperature is around 580 °C reduced. Combining the results of the cycling experiments and NH_3-TPD analysis, it is clear that the small change in conversion is related to the constant number of acid sites, while the reduced *n*-propanol selectivity is associated with the decrease in the number of acid sites whose NH_3 desorption temperature is around 580 °C. It could be further confirmed that the effect of acid amount and specific-intensity acid proportion on glycerol conversion and *n*-propanol selectivity were consistent with previous reports.

4. Conclusions

Pt-based catalysts were prepared through a facile and inexpensive process; they exhibited good selectivities for *n*-propanol. The mole ratio of Zr/Al in the catalysts can significantly affect glycerol conversion and *n*-propanol selectivity. In fact, the influence of the Zr/Al mole ratio on the reaction is attributed to the changes in the acidity of the catalyst surface; the total acid content on the catalyst surface affects the conversion of glycerol. Acid strength can affect the degree of dehydroxylation of glycerol and strong acid sites promote deep dehydration of glycerol to form propanol (including *n*-propanol and *i*-propanol). The selectivity for *n*-propanol may be related to the percentage of specific-intensity acid sites and Pt particle size. The 2.5%$Pt/Zr_{0.7}Al_{0.3}O_y$ catalyst with a Zr/Al mole ratio of 7:3 has the highest selectivity for *n*-propanol and better glycerol conversion. After optimization of the reaction conditions, 81.2% of glycerol conversion and 86.3% of *n*-propanol selectivity could be obtained with this catalyst.

References

[1] X. L. Luo, X. M. Ge, S. Q. Cui, Y. B. Li, *Bioresour. Technol.*, **2016**, 215, 144–154.
[2] D. G. Lahr, B. H. Shanks, *J. Catal.*, **2005**, 232, 386–394.
[3] S. H. Lee, D. J. Moon, *Catal. Today*, **2011**, 174, 10–16.
[4] L. Z. Qin, M. J. Song, C. L. Chen, *Green Chem.*, **2010**, 12, 1466–1472.
[5] A. Bienholz, F. Schwab, P. Claus, *Green Chem.*, **2010**, 12, 290–295.
[6] C. W. Liu, C. H. Zhang, S. L. Hao, S. K. Sun, K. K. Liu, J. Xu, Y. W. Zhu, Y. W. Li, *Catal. Today*, **2016**, 261, 116–127.
[7] J. Wang, X. C. Zhao, N. Lei, L. Li, L. L. Zhang, S. T. Xu, S. Miao, X. L. Pan, A. Q. Wang, T. Zhang, *ChemSusChem*, **2016**, 9, 784–790.
[8] Z. L. Yuan, J. H. Wang, L. N. Wang, W. H. Xie, P. Chen, Z. Y. Hou, X. M. Zheng, *Bioresour. Technol.*, **2010**, 101, 7088–7092.
[9] X. C. Zhao, J. Wang, M. Yang, N. Lei, L. Li, B. L. Hou, S. Miao, X. L. Pan, A. Q. Wang, T. Zhang, *ChemSusChem*, **2017**, 10, 819–824.
[10] C. T. Q. Mai, F. T. T. Ng, *Catal. Today*, **2017**, 291, 195–203.
[11] L. Yu, J. Yuan, Q. Zhang, Y. M. Liu, H. Y. He, K. N. Fan, Y. Cao, *ChemSusChem*, **2014**, 7, 743–747.
[12] S. H. Zhu, Y. L. Zhu, S. L. Hao, H. Y. Zheng, T. Mo, Y. W. Li, *Green Chem.*, **2012**, 14, 2607–2616.
[13] H. Ren, Y. Chen, Y. L. Huang, W. H. Deng, D. G. Vlachos, J. G. Chen, *Green Chem.*, **2014**, 16, 761–769.
[14] V. Zacharopoulou, E. S. Vasiliadou, A. A. Lemonidou, *Green Chem.*, **2015**, 17, 903–912.
[15] S. D. Blass, R. J. Hermann, N. E. Persson, A. Bhan, L. D. Schmidt, *Appl. Catal. A*, **2014**, 475, 10–15.
[16] Z. J. Wu, K. Q. Zhao, S. H. Ge, Z. Qiao, J. S. Gao, T. Dou, A. C. K. Yip, M. H. Zhang, *ACS Sustainable Chem. Eng.*, **2016**, 4, 4192–4207
[17] D. L. Sun, Y. Yamada, S. Sato, *Appl. Catal. B*, **2015**, 174–175, 13–20.
[18] S. S. Priya, V. P. Kumar, M. L. Kantam, S. K. Bhargava, S. Periasamy, K. V. R. Chary, *Appl. Catal. A*, **2015**, 498, 88–98.
[19] M. Guo, X. J. Gao, W. S. Dong, *Appl. Chem. Ind.*, **2016**, 45, 278–282.
[20] M. Signoretto, E. Ghedini, F. Menegazzo, G. Cerrato, V. Crocellà, C. L. Bianchi, *Microporous Mesoporous Mater.*, **2013**, 165, 134–141.
[21] N. R. Shiju, M. Anilkumar, W. F. Hoelderich, D. R. Brown, *J. Phys. Chem. C*, **2009,** 113, 7735–7742.
[22] C. Tagusagawa, A. Takagaki, A. Iguchi, K. Takanabe, J. N. Kondo, K. Ebitani, S. Hayashi, T. Tatsumi, K. Domen, *Angew. Chem. Int. Ed.*, **2010**, 49, 1128–1132.
[23] C. Tagusagawa, A. Takagaki, A. Iguchi, K. Takanabe, J. N. Kondo, K. Ebitani, T. Tatsumi, K. Domen, *Chem. Mater.*, **2010**, 22, 3072–3078.
[24] L. Wang, H. H. Wan, S. H. Jin, X. Chen, C. Li, C. H. Liang, *Catal. Sci. Technol.*, **2015**, 5, 465–474.
[25] J. He, H. Li, Y. M. Lu, Y. X. Liu, Z. B. Wu, D. Y. Hu, S. Yang, *Appl. Catal. A*, **2016**, 510, 11–19.
[26] H. Mustu, S. Yasyerli, N. Yasyerli, G. Dogu, T. Dogu, P. Djinović, A. Pintar, *Int. J. Hydrogen Energy*, **2015**, 40, 3217–3228.

Graphical Abstract

Chin. J. Catal., 2018, 39: 1121–1128 doi: 10.1016/S1872-2067(18)63068-2

Glycerol hydrogenolysis to *n*-propanol over Zr-Al composite oxide-supported Pt catalysts

Chuang Li, Bo He, Yu Ling, Chi-Wing Tsang, Changhai Liang *
Dalian University of Technology;
Technological and Higher Education Institute of Hong Kong

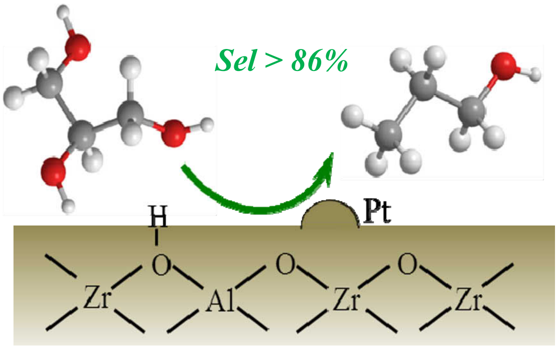

Zr-Al mixed oxide-supported Pt catalysts with different Zr/Al mole ratios were synthesized by an impregnation method and used in the selective hydrogenolysis of glycerol to *n*-propanol with high activity, selectivity, and absolute reusability.

[27] X. Q. Gao, Y. Z. Wang, H. T. Li, Y. X. Zhao, *J. Mol. Catal. (China)*, **2011**, 25, 49–54.
[28] J. L. Chen, X. Chen, X. K. Wang, M. He, M. Ji, T. X. Cai, *Chin. J. Catal.*, **2009**, 30, 619–623.
[29] J. H. Li, P. Ao, X. Q. Li, X. S. Xu, X. X. Xu, X. Gao, X. H. Yan, *Acta Phys. Chim. Sin.*, **2015**, 31, 173–180.
[30] A. Sinhamahapatra, N. Sutradhar, S. Pahari, H. C. Bajaj, A. B. Panda, *Appl. Catal. A*, **2011**, 394, 93–100.
[31] P. Bhanuchander, S. S. Priya, V. P. Kumar, S. Hussain, N. Pethan-Rajan, S. K. Bhargava, K. V. R. Chary, *Catal. Lett.*, **2017**, 147, 845–855.
[32] A. Wawrzetz, B. Peng, A. Hrabar, A. Jentys, A. A. Lemonidou, J. A. Lercher, *J. Catal.*, **2010**, 269, 411–420.
[33] J. Oh, S. Dash, H. Lee, *Green Chem.*, **2011**, 13, 2004–2007.

Zr-Al复合氧化物负载Pt催化甘油氢解制正丙醇

李　闯[a], 何　博[a], 凌　雨[a], 曾志荣[b], 梁长海[a,*]
[a]大连理工大学化工学院先进材料和催化工程实验室, 辽宁大连116024
[b]香港高等教育科技学院, 科技学院, 香港50011

摘要: 近年来,甘油氢解的研究主要集中在生成1,2-丙二醇和1,3-丙二醇二元醇. 与二元醇相比,正丙醇也是一种昂贵的化学品,用过量的甘油直接氢解合成高选择性的正丙醇将是一个非常好的生产途径. 因为铂金属具有较强的断C–O键的能力, 所以甘油氢解制正丙醇的催化剂主要采用铂作为活性组分. 本文以铂为活性组分, 采用浸渍法将其负载到不同Zr/Al比的Zr-Al复合氧化物上制得2.5%Pt/$Zr_xAl_{1-x}O_y$催化剂, 并将其应用到甘油氢解反应中, 探讨了Zr/Al比对甘油氢解制正丙醇反应性能的影响.

表征结果发现, 锆铝混合氧化物经过400 ^{o}C焙烧后为无定形态的复合金属氧化物, 载体中无单相氧化锆或氧化铝存在. 随着锆含量增加, 催化剂酸性位点向强酸方向移动. 不同Zr/Al比的锆铝混合氧化物负载铂催化剂的评价结果发现, 甘油转化率随催化剂中铝含量增加而增大; 锆铝比大于5:5时, 丙醇 (正丙醇+异丙醇) 的选择性很高, 普遍大于87%; 锆铝比至7:3时, 正丙醇选择性最高. 通过X射线衍射、CO化学吸附、H_2程序升温还原、吡啶吸附、氨气程序升温脱附等方法对催化剂进行了表征, 发现随着锆铝混合氧化物中锆含量的增加, 催化剂的酸性位点向强酸方向移动, 调变Zr/Al比促进了铂颗粒的分散, 实现了催化剂表面酸量和强酸位点的定向调控. 当锆铝比增加至7:3时, 催化剂的强酸位点占总酸含量的91.2%. 对比催化剂酸性分析和反应结果可知, 催化剂表面的总酸含量高有助于甘油转化; 强酸位点有助于甘油深度脱水生成丙醇; 正丙醇的选择性则可能与NH_3脱附温度在580 ^{o}C处的强酸位和较大的Pt颗粒有关. 当Zr/Al比为7:3时, 催化剂表面强酸位点占91.2%, 而强酸位点的增加有助于甘油的深度脱水形成正丙醇. 因此, 以10%甘油水溶液为原料, 在240 ^{o}C和6.0 MPa初始氢气压力条件下反应8 h, 甘油转化率和正丙醇的选择性分别达到81.2%和86.3%. 催化剂经过5次循环使用后, 甘油转化率和丙醇 (正丙醇+异丙醇) 选择性几乎不变, 但正丙醇的选择性略有降低. 使用5次后的催化剂表面的总酸量变化不大, 但酸分布变化较大, 即强酸比例下降. 可见, 催化剂活性变化小是由于其表面酸量变化不大, 而正丙醇选择性下降与强酸位点比例下降有关.

关键词: 甘油氢解; 正丙醇; 铂催化剂; 锆铝复合氧化物; 锆/铝比

收稿日期: 2018-01-29. 接受日期: 2018-03-22. 出版日期: 2018-06-05.

*通讯联系人. 电话/传真: (0411)84986353; 电子信箱: changhai@dlut.edu.cn

基金来源: 国家自然科学基金 (21573031, 21373038); 大连市优秀人才支持计划 (2016RD09); 辽宁省博士启动基金 (20170520395).
本文的电子版全文由Elsevier出版社在ScienceDirect上出版(http://www.sciencedirect.com/science/journal/18722067).